Polymer 50 (2009) 3470–3477

Contents lists available at ScienceDirect

Polymer

journal homepage: www.elsevier.com/locate/polymer

# Synthesis of photo- and pH-responsive composite nanoparticles using a two-step controlled radical polymerization method

Haike Feng [a,b], Yi Zhao [a], Maxime Pelletier [a], Yi Dan [b,*], Yue Zhao [a,*]

[a] Département de chimie, Université de Sherbrooke, Sherbrooke, Québec, Canada J1K 2R1
[b] State Key Laboratory of Polymer Materials Engineering of China, Polymer Research Institute, Sichuan University, Chengdu 610065, China

ARTICLE INFO

*Article history:*
Received 13 March 2009
Received in revised form
30 May 2009
Accepted 6 June 2009
Available online 12 June 2009

*Keywords:*
Polymer nanoparticles
Controlled radical polymerizations
Stimuli-responsive polymers

ABSTRACT

We present a versatile synthetic method for photo- and pH-sensitive composite nanoparticles using a combined use of reversible addition-fragmentation chain transfer (RAFT) and atom transfer radical polymerization (ATRP). Crosslinked nanoparticles of a random copolymer composed of methyl methacrylate (MMA), 4-vinylbenzyl chloride (VBC) and divinylbenzene (DVB) were first synthesized using RAFT miniemulsion polymerization in aqueous solution. This was followed by solvent exchange through extraction and dialysis that allowed the nanoparticles to be transferred to and highly swollen in an organic solvent (anisole or THF). By dissolving a monomer of a stimuli-responsive polymer in the solution, subsequent ATRP grafting polymerization could be initiated by halide groups on the swollen nanoparticle, resulting in larger composite nanoparticles. Photosensitive poly(*1*-pyrenylmethyl methacrylate) (PPyMA) and pH-sensitive poly(dimethylaminoethyl methacrylate) (PDMAEMA) were incorporated in the composite nanoparticles, and their photo- and pH-responsive behaviors were investigated. With this method, monomers soluble in organic solvents can be used in conjunction with emulsion polymerization in aqueous solution to design functional composite nanoparticles.



## 1. Introduction

Much effort has been devoted to the use of emulsion polymerization to prepare composite latex particles that combine properties of more than one polymer. The most used method consists in polymerizing a first monomer in aqueous solution, which leads to the formation of seed particles, and then adding a second monomer followed by its polymerization [1–5]. This procedure allows for the formation of core-shell particles of two polymers, with the actual morphology controlled by thermodynamic and kinetic parameters [6]. For instance, to reduce the interfacial tension between two immiscible polymers A and B, methods were developed in which a small number of graft [7] or block copolymer [6] composed of A and B can be formed during the reaction that acts as a compatibilizing agent for the two constituent polymers. However, this method generally requires that the two monomers be in the liquid form, which limits the number of usable monomers and renders the synthesis of stimuli-responsive composite nanoparticles difficult, because, for example, most monomers for photo-responsive polymers are solid under ambient conditions. Recent efforts in exploiting the controlled radical polymerizations offer possible solutions to this problem. Among many reports, Jhaveri et al. showed that particles of a polymer bearing bromine groups could be prepared using surfactant-free emulsion polymerization, collected and redispersed in an organic solvent due to the highly crosslinked nature (using a trimethacrylare monomer as the crosslinker); with bromine groups exposed on the surface, surface-initiated atom transfer radical polymerization (ATRP) could be used to graft a second polymer resulting in core-shell nanoparticles [8]. Zhang and Stöver used precipitation copolymerization to prepare lightly crosslinked and thus swellable microspheres that, after modification to introduce bromine groups, were served as ATRP macroinitiators to graft a second polymer from an outer layer and the surface of the microspheres (diameter ~ 4 μm for the composite particles) [9]. In this paper, we report a modified version inspired by these approaches, which is based on the use of swellable nanoparticles (not microspheres) to graft a second polymer from the inside, and show that it is a general and versatile method for the synthesis of photo- and pH-sensitive polymer composite nanoparticles.

The approach is schematically illustrated in Fig. 1a. Firstly, a reversible addition–fragmentation chain transfer (RAFT)

* Corresponding authors.
*E-mail addresses:* yue.zhao@usherbrooke.ca, danyi@scu.edu.cn (Y. Dan).

0032-3861/$ – see front matter © 2009 Elsevier Ltd. All rights reserved.
doi:10.1016/j.polymer.2009.06.017

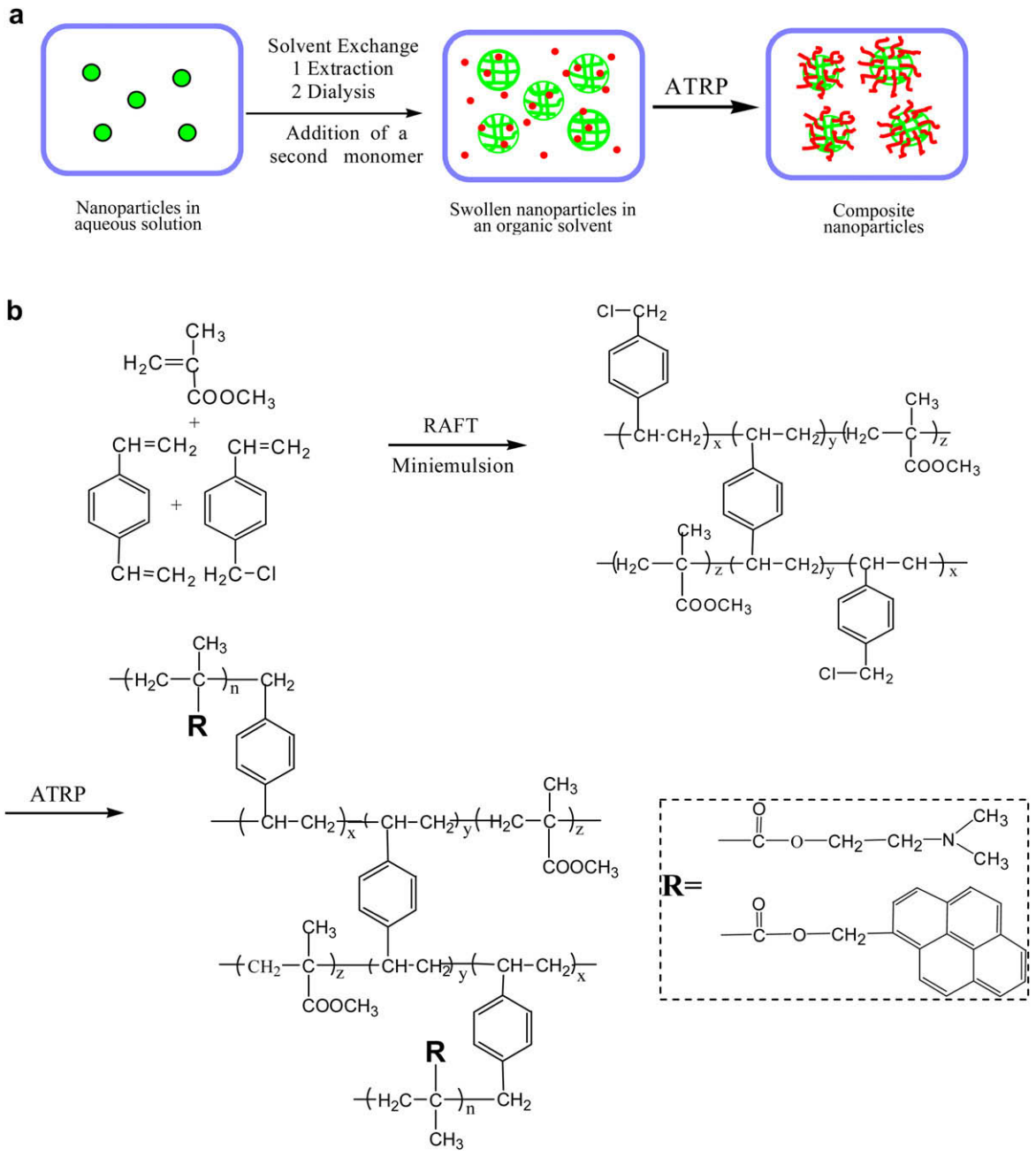


**Fig. 1.** (a) Schematic illustration of the synthetic approach based on solvent exchange and swelling of the seed nanoparticles prior to grafting polymerization. (b) General reaction scheme showing chemical structures of the stimuli-responsive composite nanoparticles.

miniemulsion polymerization is carried out in aqueous solution to produce crosslinked nanoparticles containing halide groups. This is followed by a solvent exchange process through extraction and dialysis against a chosen organic solvent, leading to solubilized and highly swollen nanoparticles. Then a second monomer is dissolved in the solution for polymerization through ATRP. Due to the swelling of the nanoparticles that exposes halide groups to the reactive solution, the ATRP is expected to start not only from the surface but also from the inside of the nanoparticles. In this way the resultant composite nanoparticles should have the second polymer emanate from the interior to surface. Given that the two polymers are immiscible, microphase separation should occur in the graft copolymer and allows for the compartmentalization of the nanoparticles. To demonstrate this method, we prepared photo- and pH-sensitive composite nanoparticles. As shown in Fig. 1b, the initial polymerization (RAFT miniemulsion) of methyl methacrylate (MMA), 4-vinylbenzyl chloride (VBC) and divinylbenzene (DVB) gives crosslinked nanoparticles dispersed in aqueous solution; after their transfer to and swelling in an organic solvent containing a second monomer, the subsequent polymerization (ATRP), enabled by VBC units [10–12], results in grafts of either photosensitive poly(*1*-pyrenylmethyl methacrylate) (PPyMA) or pH-sensitive poly-(dimethylaminoethyl methacrylate) (PDMAEMA). Note that although the crosslinked nanoparticles could be prepared using normal emulsion polymerization, RAFT was chosen with the purpose of investigating the combined use of two controlled radical polymerization methods in preparing such composite functional nanoparticles.

**Table 1**
Conditions for RAFT miniemulsion polymerization.

| Sample | Water (g) | MMA (g) | DVB (g) | VBC (g) | KPS (g) | Hexadecane (g) | Brij98 (g) | CPDB (g) | Stirring Speed (rpm) | $D_H^{DLS}$ (nm) | $D^{SEM}$ (nm) |
|---|---|---|---|---|---|---|---|---|---|---|---|
| 1 | 10 | 0.860 | 0.910 | 0 | 0.027 | 0.05 | 0.5 | 0.066 | 1000 | 120 | 80 |
| 2 | 8 | 0.750 | 0.078 | 0.44 | 0.027 | 0.05 | 0.5 | 0.066 | 600 | 352 | 180 |
| 3 | 10 | 0.750 | 0.078 | 0.44 | 0.027 | 0.05 | 0.5 | 0.066 | 700 | 319 | 125 |
| 4 | 10 | 0.750 | 0.078 | 0.67 | 0.027 | 0.06 | 0.6 | 0.066 | 600 | 338 | – |
| 5 | 10 | 0.375 | 0.078 | 0.67 | 0.027 | 0.06 | 0.6 | 0.066 | 800 | 230 | – |

$D_H^{DLS}$, Hydrodynamic diameter determined by DLS; $D^{SEM}$, average diameter determined by SEM; MMA, methyl methacrylate (monomer); DVB, divinylbenzene (crosslinker); VBC, vinylbenzyl chloride (ATRP initiator); KPS, potassium persulfate (initiator); Brij98, polyoxyethylene (20) oleyl ether (surfactant); Hexadecane (co-surfactant); CPDB, 2-(2-Cyanopropyl) dithiobenzoate (chain transfer agent).

## 2. Experimental section

### 2.1. Materials

All chemicals were purchased from Aldrich. Methyl methacrylate (MMA, 98%), divinylbenzene (DVB, 80%), 4-vinylbenzyl chloride (VBC, 90%) and 2-(dimethylamino) ethyl methacrylate (DMAEMA, 99%) were passed through a basic alumina column prior to use. 1-Pyrenylmethyl methacrylate (PyMA) was synthesized using a reported method [13]. Tetrahydrofuran (THF, 99%) was distilled from sodium benzophenone. Anhydrous anisole (99.7%) and dichloromethane (DCM, 99.5%) were used received. Copper(I) bromide (CuBr, 99.99%), N, N, N′, N′N″- pentamethyldiethylenetriamine (PMDETA, 99%), potassium persulfate (KPS, 99.99%), polyoxyethylene (20) oleyl ether (Brij98, 99%) and hexadecane were used without further purification. 2-(2-Cyanopropyl) dithiobenzoate (CPDB) was synthesized using a literature method [14].

### 2.2. Preparation of crosslinked nanoparticles using RAFT miniemulsion polymerization

Crosslinked nanoparticles bearing ATRP initiating sites (VBC units) were first synthesized using RAFT miniemulsion polymerization in aqueous solution. An example of reaction is detailed as follows. KPS (27 mg, 0.1 mmol), Brij98 (0.5 g, 0.43 mmol) were dissolved in 10 g of deionized water (0.56 mol) in a 25 mL round-bottom flask. CPDB (66 mg, 0.3 mmol) was dissolved in a solution of VBC (0.44 g, 2.9 mmol), DVB (0.078 g, 0.6 mmol), hexadecane (0.05 g, 0.22 mmol) and MMA (0.75 g, 8.7 mmol). Then, the liquid mixture of monomers containing the chain transfer agent (CPDB) was added dropwise into the aqueous solution at room temperature under nitrogen atmosphere. After 10 min sonification, the flask was placed in a thermostat oil bath at 70 °C and the reaction last 2 h. The resulting nanoparticles were purified and transferred to an organic solvent through a solvent exchange process as described below.

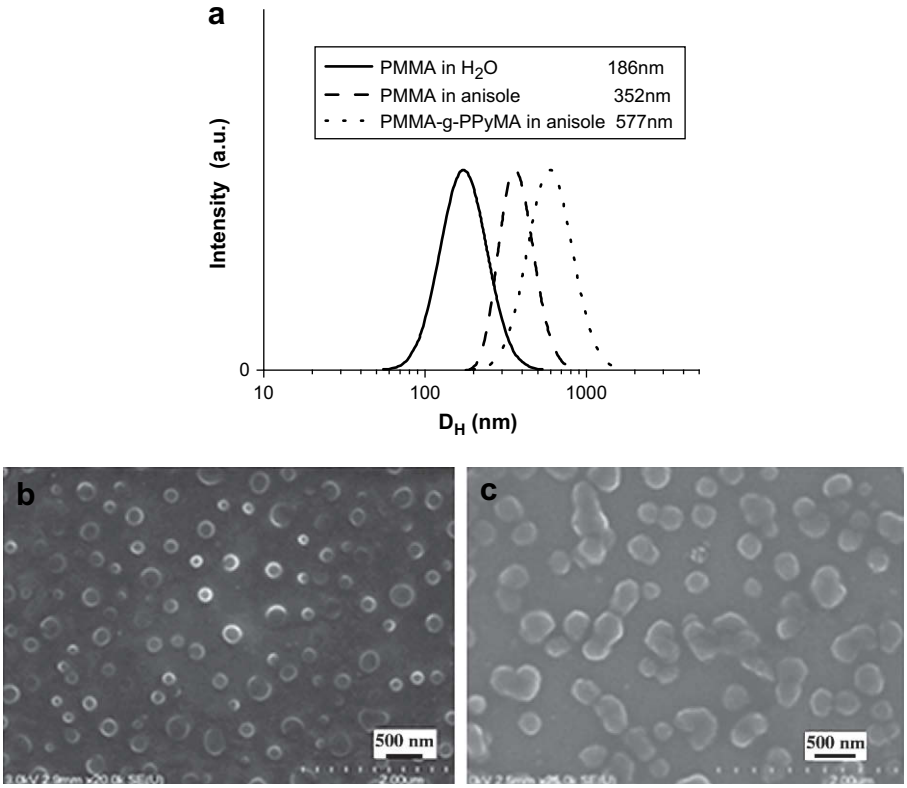


**Fig. 2.** (a) Change in the distribution of hydrodynamic diameters, (b) SEM image of PMMA nanoparticles cast from an anisole solution, and (c) SEM image of the composite nanoparticles of PMMA-*g*-PPyMA obtained after ATRP grafting in the anisole solution.

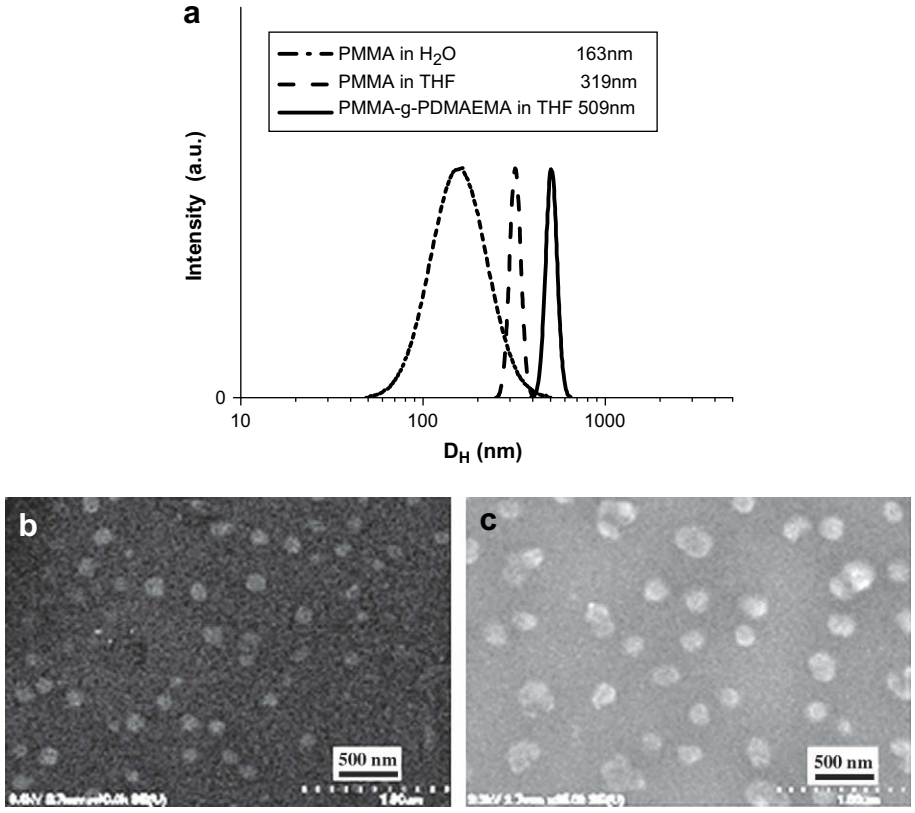


**Fig. 3.** (a) Change in the distribution of hydrodynamic diameters, (b) SEM image of PMMA nanoparticles cast from a THF solution, and (c) SEM image of the composite nanoparticles PMMA-*g*-PDMAEMA obtained after ATRP grafting in the THF solution.

### 2.3. Solvent exchange

Following the miniemulsion polymerization, the aqueous solution was poured into a solvent of DCM/$H_2O$ (5/1, v/v) and the mixture was stirred for 30 min. After it was laid for 1 h, the separated aqueous phase (top layer) containing the surfactant Brij98 and initiator KPS was removed, while the organic phase (bottom layer) containing the crosslinked nanoparticles, unreacted monomers and hexadecane (co-surfactant) was collected. Following evaporation of most DCM at room temperature, the solution was further purified by dialysis against THF for one week to remove unreacted monomers and possible surfactant molecules solubilized in dichloromethane. As described below, for the ATRP grafting of DMAEMA at 60 °C, THF was the solvent for the second monomer. However, for the grafting of PyMA at 90 °C, THF was replaced by anisole by evaporation followed by dialysis against anisole.

### 2.4. Synthesis of composite nanoparticles using ATRP

After crosslinked nanoparticles bearing chlorine groups (initiating sites) were solubilized and highly swollen in THF or anisole, stimuli-responsive composite nanoparticles could be prepared by grafting either photoactive PPyMA or pH-sensitive PDMAEMA through ATRP. For each of the two composite nanoparticles, a typical example of reaction conditions is given.

(1) *Grafting of PPyMA*: Cu(I)Br (13.68 mg, 0.095 mmol), PMDETA (32.8 mg, 0.19 mmol) and PyMA (0.86 g, 2.85 mmol) were first dissolved in 10 mL of anisole; the solution was then mixed with 10 mL of an anisole solution containing ~60 mg of swollen nanoparticles (sample 2 in Table 1) in a 25 mL round-bottom flask. The reaction mixture was degassed three times using the freeze–pump–thaw procedure and sealed under vacuum. After 30 min of stirring at room temperature, the flask was placed in an oil bath preheated to 90 °C and the reaction last for 24 h. With the nanoparticles dispersed in solution, the copper salts could not be removed by passing the solution through a neutral alumina column. Instead, the solution was laid at rest to allow the precipitation of the catalyst. Then diluted solution was further purified by dialysis against THF to remove unreacted monomers and remaining ATRP catalyst. $^1$H-NMR ($CDCl_3$), $\delta$ (ppm): 8.19–7.99 (broad, 9H, aromatic pyrene), 5.89 (broad, 2H, –$CH_2O$–, pyrene), 3.78 (s, 3H, $CH_3O$–, MMA), 1.97 (s, 3H, $CH_3$, MMA).

**Table 2**
Conditions for ATRP polymerization.

| Sample | Macroinitiator (mg) | CuBr (mg) | PMDETA (mg) | Monomer (g) | $D_H^{DLS}$ (nm) | $D^{SEM}$ (nm) |
|---|---|---|---|---|---|---|
| 6 | 64 (Sample 3) | 14.40 | 34.53 | 0.785 (DMAEMA) | 509 | 223 |
| 7 | 60 (Sample 2) | 13.68 | 32.80 | 0.860 (PyMA) | 577 | 270 |
| 8 | 45 (Sample 4) | 14.40 | 34.53 | 0.785 (DMAEMA) | 536 | — |
| 9 | 45 (Sample 5) | 14.40 | 34.53 | 0.785 (DMAEMA) | 439 | — |

$D_H^{DLS}$, Hydrodynamic diameter determined by DLS; $D^{SEM}$, average diameter determined by SEM; CuBr (catalyst of ATRP); PMDETA, ligand of ATRP.

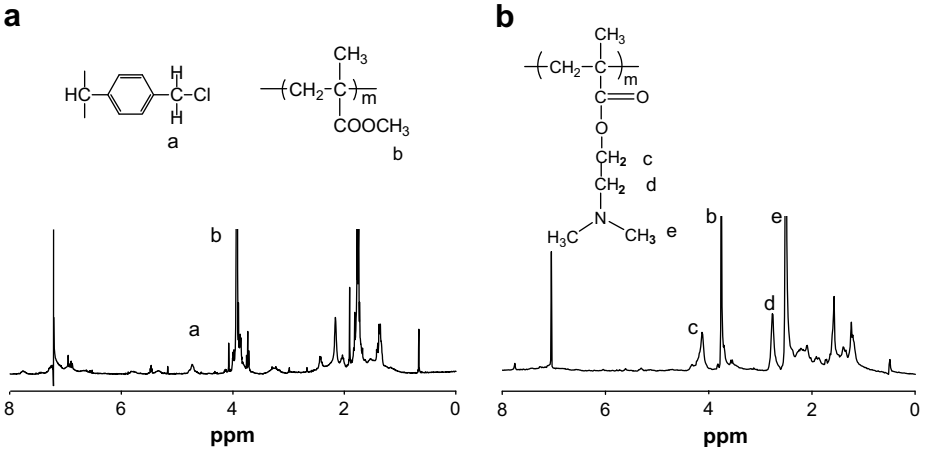


**Fig. 4.** $^1$H-NMR spectra of (a) nanoparticles PMMA and (b) composite nanoparticles PMMA-*g*-PDMAEMA in $CDCl_3$.

(2) *Grafting of PDMAEMA*: Cu(I)Br (14.40 mg, 0.1 mmol), PMDETA (34.53 mg, 0.2 mmol) and DMAEMA (0.785 g, 5.0 mmol) were dissolved in THF; the solution was mixed with 5 mL of a THF solution containing ~64 mg of nanoparticles (sample 3 in Table 1). The reaction mixture was degassed three times using the freeze–pump–thaw procedure and sealed under vacuum. After 30 min of stirring at room temperature, the flak was placed in an oil bath preheated to 60 °C and the reaction last 24 h. The resulting composite nanoparticles were purified by using the procedure described above. $^1$H-NMR ($CDCl_3$), $\delta$ (ppm): 4.09 (t, 2H, $CH_2O$–, DMAEMA), 3.78 (s, 3H, $CH_3O$–, MMA), 2.62 (t, 2H, $CH_2N$–, DMAEMA), 2.21 (s, 6H, $CH_3N$–, DMAEMA), 1.97 (s, 3H, $CH_3$–, MMA).

### 2.5. Characterizations

$^1$H-NMR spectra were recorded on a Bruker Spectrometer (300 MHz, AC 300). Dynamic light scattering (DLS) experiments were performed using a Brookhaven goniometer (BI-200) equipped with a highly sensitive avalanche photodiode detector (BI-APD), a digital correlator (TurboCorr) that calculates the photon intensity autocorrelation function $g^2(t)$, a helium–neon laser ($\lambda = 632.8$ nm), and a thermostat sample holder. The measurements were made at scattering angle of 90°, and the distribution of hydrodynamic diameters ($D_H$) of nanoparticles was obtained by a cumulant and CONTIN analysis. UV-vis absorption and steady-state fluorescence emission spectra were recorded using a UV-vis (Varian Cary50 Bio) and a fluorescence spectrophotometer (Varian Cary Eclipse), respectively. The excitation and emission slit widths were set at 5 nm, and the scan rate was 10 nm s$^{-1}$. For UV irradiation of photosensitive nanoparticles, a solution (~3 mL) was filled in a standard quartz cell (1 cm$^2$ cross section) under mild stirring, while UV light (365 nm, 500 mW cm$^{-2}$, produced from a Novacure spot curing system) was applied vertically from the top of the cell. SEM observations were carried out using a Hitachi S-4700 Emission Gun Scanning Electron Microscope; samples were prepared by deposing one drop of the nanoparticle solution on a silicon wafer, followed by drying at room temperature. A Hitachi H-7500 transmission electron microscope (TEM) operating at 80 kV was used to examine the morphology. For sample preparation, composite nanoparticles were embedded in the cured epoxy resin, froze to −120 °C and microtomed. The slices were then placed on warm water (35 °C) and transferred from the water surface to 400-mesh Cu grids. The grids were dried and placed in a chamber with $RuO_4$ for 15 min, removed, and examined.

## 3. Results and discussion

To facilitate the discussion, the initial nanoparticles obtained after the RAFT miniemulsion polymerization of the mixture of MMA, DVB and VBC are denoted as PMMA hereafter, while the composite nanoparticles after the PMMA-initiated ATRP of PyMA and DMAEMA are referred to as PMMA-*g*-PPyMA and PMMA-*g*-PDMAEMA, respectively. The PMMA sample 2 in Table 1 was used to polymerize PyMA in anisole, while the PMMA sample 3 was used to polymerize DMAEMA in THF. The large swelling of PMMA after the solvent exchange to either anisole or THF and the efficient grafting of PPyMA and PDMAEMA by the swollen particle-initiated ATRP were confirmed by DLS measurements and SEM observation. Fig. 2 shows the results for PMMA-*g*-PPyMA. According to DLS, the average hydrodynamic diameter ($D_H$) of PMMA nanoparticles in aqueous solution is about 186 nm; after transfer into anisole, $D_H$ increases to 352 nm, indicating a large swelling of the nanoparticles. Following the ATRP of PyMA dissolved in the anisole solution, the average $D_H$ further increases to 577 nm for PMMA-*g*-PPyMA, showing the successful grafting of the second polymer and the formation of the composite nanoparticles. SEM images show the sizes of dried nanoparticles before and after the ATRP and confirm that the composite nanoparticles have a larger average size than the initial PMMA nanoparticles. At the dried state, the nanoparticles are much smaller than in the anisole solution, revealing again their highly swellable nature and thus allowing polymerization of the second monomer from the inside of the initial nanoparticles.

Similar conclusions can be drawn from Fig. 3 presenting the results of PMMA-*g*-PDMAEMA, for which the ATRP was carried out in THF. While the initial PMMA has an average $D_H$ of 163 nm in aqueous solution with a similar distribution width to the sample in Fig. 2a, a different condition was purposely used for the solvent exchange. By using a dialysis bag with a much greater cutoff molecular weight (50,000 compared to 1000 for the results in Fig. 2a), the dialysis against THF removed smaller PMMA so that the swollen nanoparticles in THF ($D_H \sim 319$ nm) displayed a much narrower distribution of $D_H$ prior to the ATRP of DMAEMA. After the grafting of PDMAEMA, the average size of the composite nanoparticles increased to $D_H \sim 509$ nm, while retaining a narrow distribution of sizes. This result shows that by fractioning the PMMA nanoparticle initiator, it is possible to prepare uniformly sized composite nanoparticles.

Judging from the change in $D_H$, the grafting of both PPyMA and PDMAEMA on PMMA resulted in a dramatic increase in the hydrodynamic volume of the polymer nanoparticles (Figs. 2 and 3).

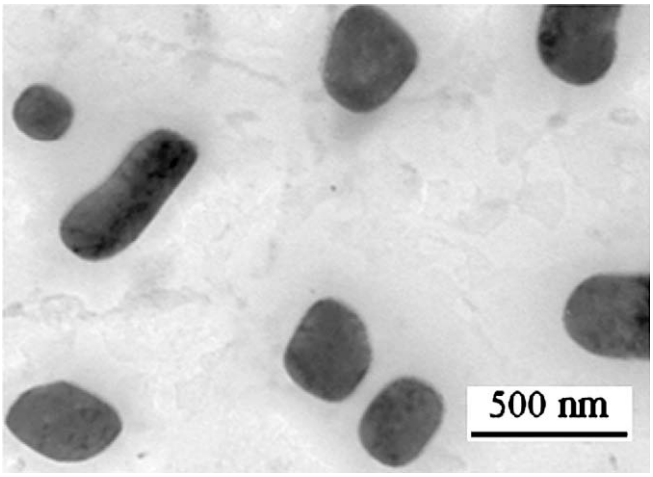


**Fig. 5.** Cross-sectional TEM image of composite nanoparticles PMMA-*g*-PPyMA.

It is unlikely that this increase was only due to the grafting of either PPyMA or PDMAEMA chains on the surface of PMMA nanoparticles. Considering that the grafting polymerization takes place from inside the swollen nanoparticles, the resulting composite nanoparticles could have a different solubility in the used organic solvent that results in an increased swelling of the crosslinked nanoparticles. This assumption is qualitatively supported by the observed change in $D_H$ of the composite nanoparticles in response to pH change or a photoreaction, as will be shown later. In other words, the large increase in $D_H$ of the composite nanoparticles could be caused by an enhanced particle swelling in addition to the grafting of the second polymer.

Table 1 shows the conditions used to prepare different PMMA by RAFT miniemulsion polymerization. It is known that the size of polymer particles prepared by using this method is determined by factors such as the molar ratio of MMA to water, the molar ratio of surfactant to MMA and the stirring speed. Under the used conditions, PMMA nanoparticles with slightly different sizes were obtained. Summarized in Table 2 are the conditions used to synthesize the composite nanoparticles with two PMMA initiators (samples 2 and 3 in Table 1). In all cases, it was difficult to determine precisely the actual composition of the composite nanoparticles by $^1$H-NMR because they could only be swollen in solution so that the resonance signals of less-well-solvated regions, likely to be near the particle center, appear weak and broad. Nevertheless, an estimate could be done from the NMR measurements. As an example, Fig. 4 shows the spectra of PMMA (sample 3 in Table 1) and PMMA-*g*-PDMAEMA (sample 6 in Table 2). For the nanoparticle initiator, the comparison of the integrals of the characteristic resonance peaks of MMA at 3.78 ppm and VBC at 4.6 ppm suggests that the amount of VBC bearing the ATRP initiating sites be about 5 wt% of that of MMA (Fig. 4a). Even though the content of DVB could not be determined with certainty, the weak resonance signals of phenyl protons around 7 ppm, overlapped with those of VBC, suggests a weak crosslinking degree for the PMMA nanoparticles. The highly swollen state of the particles in organic solvents (Figs. 2 and 3) also implies a weak crosslinking degree. For the composite nanoparticle after ATRP, the grafting of PDMAEMA is indicated by the resonance peak at 4.1 ppm; the integral of this peak relative to the peak of MMA at 3.78 ppm suggests a content of ~77 wt% of PDMAEMA with respect to MMA (Fig. 4b), i.e., about 43.6% of the grafted polymer in the composite nanoparticles. Similar NMR analyses yielded ca. 44.2% of PPyMA in the composite nanoparticle of PMMA-*g*-PPyMA (sample 7). TEM was used to observe the morphology of composite nanoparticles. Fig. 5 shows a cross-sectional image of PMMA-*g*-PPyMA. A heterogeneous morphology can be noticed from the contrast, with dark regions probably belonging to PPyMA because of concentrated aromatic moieties. No core-shell morphology was observed, implying that the grafting of PPyMA could take place from the interior of the nanoparticles due to the highly swollen state in the reaction solution. Image obtained with PMMA-*g*-PDMAEMA are not clear presumably due to the difficulty in staining the microdomains (PDMAEMA has no phenyl groups).

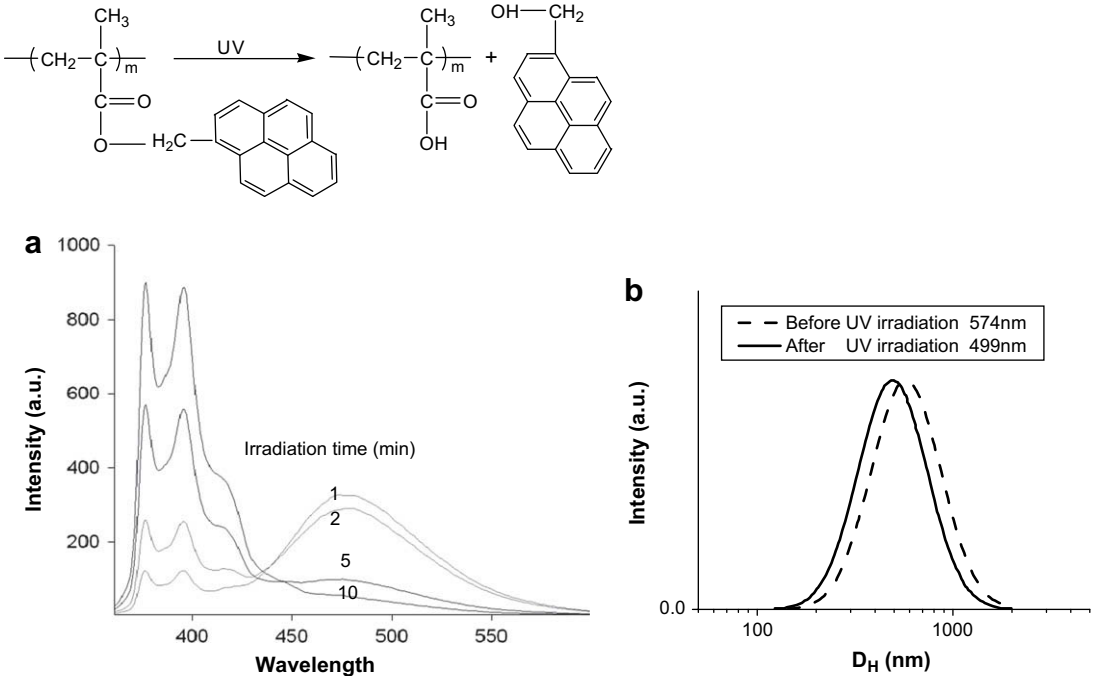


**Fig. 6.** (a) Fluorescence emission spectra ($\lambda_{ex} = 315$ nm) and (b) distribution of hydrodynamic diameters of the photosensitive composite nanoparticles PMMA-*g*-PPyMA in THF/water (90/10, w/w) before and after UV irradiation (365 nm, 500 mW/cm$^2$, 3 mL solution).

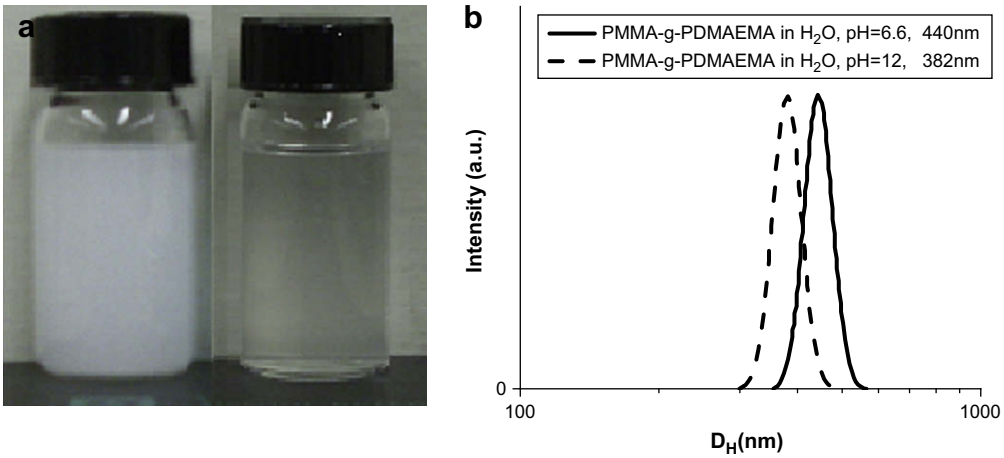


**Fig. 7.** (a) Pictures of nanoparticles PMMA (left) and composite nanoparticles PMMA-*g*-PDMAEMA (right) redispersed in water. (b) Change in the distribution of hydrodynamic diameters of PMMA-*g*-PDMAEMA in response to a change in pH.

Before presenting the results on the stimuli-responsive behaviors of the composite nanoparticles, a question can be raised: does the presence of RAFT end groups in the PMMA particles have effect on the subsequent ATRP grafting of the second polymer? Nicolay et al. investigated the use of an initiator compound comprising a trithiocarbonate moiety and two bromine chain ends for ATRP of MMA [15]. They found that depending on the ligand used for the copper catalyst, the polymerization could either proceed only through ATRP (from bromine chain ends) or through both ATRP and RAFT (from trithiocarbonate moiety). Therefore, it is possible that the residual RAFT end groups in the PMMA particles could contribute to the grafting of the second polymer under the ATRP conditions. To check this possibility, the following control test has been performed. Crosslinked nanoparticles bearing dithioester end groups but without benzyl chloride groups were first prepared through RAFT miniemulsuion polymerization, using the same conditions as for sample 3 in Table 1 except that no VBC was used as a comonomer; they were then used to conduct ATRP of DMAEMA using exactly the same conditions as for sample 6 in Table 2. The $^1$H-NMR measurement showed the grafting of about 6 wt% of PDMAEMA with respect to MMA. As compared to ~77 wt% of PDMAEMA in the composite nanoparticles prepared using sample 3 with VBC units as the ATRP initiator, this result indicates that the residual dithioester end groups in the crosslinked nanoparticles could contribute to the growth of the second polymer, but the effect was small with respect to the grafting through ATRP initiated by benzyl chloride groups. In addition to the use of an ATRP-effective catalyst, a much larger concentration of VBC side groups than dithioester end groups is likely another reason for the dominant ATRP contribution.

Using this two-step method, in principle any ATRP monomer soluble in an organic solvent can be polymerized and grafted to the initial nanoparticles, prepared using emulsion polymerization in aqueous solution, through an appropriate solvent exchange and a light crosslinking for swelling. This offers a means to design functional composite nanoparticles that, for example, respond to stimuli such as light and pH change. The two polymers grafted to PMMA nanoparticles were chosen to demonstrate this possibility. Of them, PMMA-*g*-PPyMA is photosensitive due to the photosolvolysis of pyrenylmethyl esters [16]. The photoreaction was investigated with the composite nanoparticles dissolved in a mixed solvent of THF/water (90/10 w/w) (the presence of a protic solvent is required for the photosolvolysis reaction) and by exposing the solution to a UV light (3 mL solution, UV intensity 500 mW/cm$^2$). The photoreaction is shown in Fig. 6, along with fluorescence and DLS measurement results. The photoinduced cleavage of pyrenemethanol accounts for the fluorescence emission spectral changes. Before irradiation, with excitation at 315 nm, the fluorescence emission of pyrene excimers around 478 nm is predominant, which is normal for a polymer bearing pyrene moieties as side groups (PPyMA). While with increasing the UV irradiation time, the monomer emission of pyrene at 380–410 nm becomes more and more prominent at the expense of the excimer emission, which indicates the continuous removal of pyrenemethanol from the nanoparticles into the solution (Fig. 6a). By converting pyrenylmethyl methacrylate side groups to methacrylic acid groups for PPyMA, the photoreaction changes the chemical composition of the composite nanoparticles and thus the solubility toward a given solvent. This photoinduced effect leads to a change in the average size of the nanoparticles in the solution, which can be seen from the shift of the distribution of $D_H$ as measured by DLS (Fig. 6b). The decrease in the average $D_H$ after UV irradiation corresponds to a volume contraction of the nanoparticles by about 34%.

To observe the pH-sensitivity of PMMA-*g*-PDMAEMA, the composite nanoparticles need to be dispersible in water. This indeed is the case as shown by the photos in Fig. 7a. PMMA-*g*-PDMAEMA composite nanoparticles were synthesized in THF; after drying they could be redispersed in water by sonification giving rise to a clear solution. By contrast, under the same preparation conditions, the initial PMMA nanoparticles without water-soluble PDMAEMA could not be redispersed, resulting in a turbid solution. At room temperature and pH ~ 6.6, the DLS measurement showed an average $D_H$ of 440 nm for PMMA-*g*-PDMAEMA. As expected, this size is smaller than that of nanoparticles fully solubilized in THF (509 nm, Fig. 3a), because PMMA is insoluble in water. The apparent water-solubility is clearly provided by the PDMAEMA component. However, when pH was increased to 12, the deprotonation of DMAEMA units made PDMAEMA also insoluble in water [17], resulting in a contraction of the composite nanoparticles by about 35%, with the average $D_H$ down to 382 nm.

## 4. Conclusions

In this paper, we presented a versatile method for the synthesis of photo- or pH-responsive composite nanoparticles. It started with the RAFT miniemulsion polymerization of a mixture of monomers (MMA, VBC and DVB) in aqueous solution, producing crosslinked nanoparticles stabilized by surfactants. After a solvent exchange

process via extraction and dialysis, surfactant-free nanoparticles were transferred into an organic solvent (anisole or THF), solubilized and highly swollen. By dissolving the monomer of a stimuli-responsive polymer (PyMA or DMAEMA) in the solution, the ATRP grafting polymerization of the monomers could be initiated by the initial nanoparticles, leading to composite nanoparticles of the graft copolymer. We demonstrated the efficiency and versatility of this method by introducing photosensitive PPyMA and pH-sensitive PDMAEMA into the composite nanoparticles. The interest of this method is that it provides a general means to explore many monomers in the preparation of functional (such as stimuli-responsive) composite nanoparticles in conjunction with emulsion polymerization in aqueous media. With a swollen nanoparticle initiator, the grafting of the stimuli-responsive polymer can proceed from the interior of nanoparticles (volume initiation). This also provides a way to develop multicompartment polymer nanoparticles based on the microphase separation, which differs from the well-known core-shell morphology obtained by using particle surface-initiated polymerization.

## Acknowledgements

YZ acknowledges financial support from the Natural Sciences and Engineering Research Council of Canada (NSERC) and le Fonds québécois de la recherche sur la nature et les technologies of Québec (FQRNT). YD acknowledges financial support from the National Natural Science Foundation of China (No. 20374036). HKF thanks China Scholarship Council for a scholarship. YZ is a member of the FQRNT-funded Center for Self-Assembled Chemical Structures (CSACS).

## References

[1] Xiao XC, Chu LY, Chen WM, Wang S, Li Y. Adv Funct Mater 2003;13:847.
[2] Montagne F, Mondain-Monval O, Pichot C, Elaissari A. J Polym Sci Part A Polym Chem 2006;44:2642.
[3] Li CY, Chiu WY, Don TM. J Polym Sci Part A Polym Chem 2007;45:3902.
[4] Pavlyuchenko VN, Sorochinskaya OV, Ivanchev SS, Klubin VV, Kreichman GS, Budtov VP, et al. J Polym Sci Part A Polym Chem 2001;39:1435.
[5] Ni KF, Sheibat-Othman N, Shan GR, Fevotte G, Bourgeat-Lami E. Macromolecules 2005;38:9100.
[6] Herrera V, Pirri R, Leiza JR, Asua JM. Macromolecules 2006;39:6969.
[7] Rajatapiti P, Dimonie VL, El-Aasser MS. J Macromol Sci Pure Appl Chem 1995;A32:1445.
[8] Jhaveri SB, Koylu D, Maschke D, Carter KR. J Polym Sci Part A Polym Chem 2007;45:1575.
[9] Zheng GD, Stöver HDH. Macromolecules 2002;35:7612.
[10] Xu FJ, Kang ET, Neoh KG. Macromolecules 2005;38:1573.
[11] Xu FJ, Yuan ZL, Kang ET, Neoh KG. Langmuir 2004;20:8200.
[12] Holmberg S, Holmlund P, Wilen CE, Kallio T, Sundholm G, Sundholm F. J Polym Sci Part A Polym Chem 2002;40:591.
[13] Lou X, Daussin R, Cuenot S, Duwez AS, Pagnoulle C, Detrembleur C, et al. Chem Mater 2004;16:4005.
[14] Chiefari J, Chong YK, Ercole F, Krstina J, Jeffery J, Le TPT, et al. Macromolecules 1998;31:5559.
[15] Nicolay R, Kwak Y, Matyjaszewski K. Macromolecules 2008;41:4585.
[16] Jiang J, Tong X, Zhao Y. J Am Chem Soc 2005;127:8290.
[17] Btn V, Lowe AB, Billingham NC, Armes SP. J Am Chem Soc 1999;121:4288.